

Analysis of the Electrochemical Removal of Aluminium Matrix Composites Using Multiphysics Simulation

Matthias Hackert-Oschätzchen^{*,1}, Norbert Lehnert¹, Michael Kowalick¹, Gunnar Meichsner², Andreas Schubert^{1,2}

¹Professorship Micromanufacturing Technology, Technische Universität Chemnitz, 09107 Chemnitz, Germany

²Fraunhofer Institute for Machine Tools and Forming Technology, 09126 Chemnitz, Germany
*09107 Chemnitz, Germany, matthias.hackert@mb.tu-chemnitz.de

Abstract: In the Collaborative Research Centre 692 at the Technische Universität Chemnitz several academic institutions work on aluminium matrix composites (AMCs). Such materials are investigated from development to machining. One possible method for machining AMCs is electrochemical machining. To characterise the electrochemical removal an analysing device was developed. Therefore two fully coupled 2D-models were built up with COMSOL Multiphysics to study the ECM process and to detect settings for the use of the analysing device. In the models the electric current, the non-isothermal flow and the deformed geometry interface were used. As a result of the first study suitable settings for the inlet velocity of the electrolyte and a constance of temperature were found. In the second study the anodic dissolution could be simulated. As a result a suitable feed rate for the analysing process was detected.

Keywords: Electrochemical Machining, Anodic Dissolution, Metal Matrix Composites, Aluminium Matrix Composites, analysing device, flow cell

1. Introduction

The increasing requirements on the properties of material used in modern technologies, especially in safety-related parts and components, cannot be met by the conventional metal alloys, ceramics, and polymeric materials. For example in aeronautics materials are required which have a low density to reduce mass, but also have a high stiffness. Therefore, composite materials were created as a combination of two or more physical and chemical different materials. The different materials exist as separated phases in the composite. Because of the different phases composites are difficult to machine with conventional methods such as milling. [1–3]

Aluminium matrix composites (AMCs) are investigated in several academic institutions of the Technische Universität Chemnitz, which work together in the Collaborative Research Centre 692 HALS. These materials consist of an aluminium matrix, which is reinforced by particles, e.g. SiC or Al₂O₃ with dimensions less or equal 1 µm. In the CRC 692 such materials are studied from the development process, different ways of production and machining up to potential applications. One main task is the finishing machining of AMCs by electrochemical machining (ECM).

The manufacturing technology ECM, which is based on anodic dissolution, has a slight influence on the work piece material structure and is independent of material strength and hardness. The purposes of the research are depending on the application whether to resolve the matrix specifically to uncover the particles, to resolve the whole composite or to anodize locally the aluminium. [4] For the process design, the electrochemical characteristics of the AMCs have to be analysed. For that reason an analysing device for an existing prototype system is developed. Based on this device two fully coupled models were built up with COMSOL Multiphysics. These models are used to detect settings for the use of the analysing device in a first step and to simulate the electrochemical dissolution in a second step.

2. Model design

2.1 Geometry

As mentioned in the introduction the model is based on an analysing device developed at the Technische Universität Chemnitz. Figure 1 shows the analysing device (a) and a section view (b). The device is a flow cell where the work piece will be inserted from below.

In the section view it can be seen the tool electrode made of stainless steel, the work piece and the aqueous electrolyte. The electrolyte

flows from one side to the other, e.g. from left to right. The chamber, which is highlighted green, is made of insulating plastic. The area selected for the model is surrounded by a red line in image (b).

The model geometry built up in COMSOL Multiphysics is shown in figure 2.

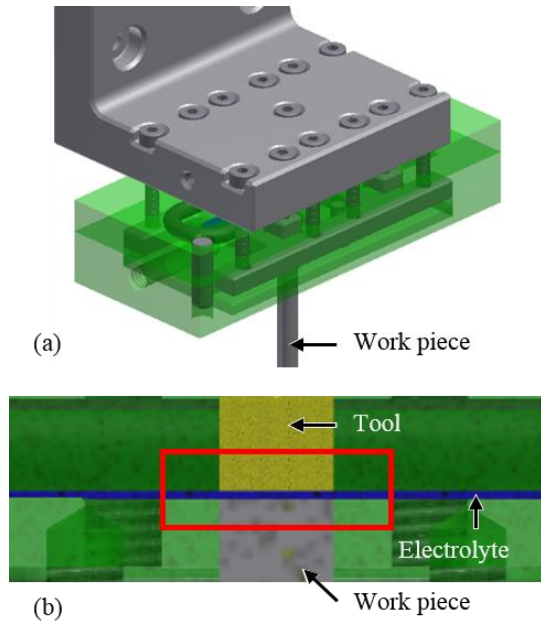


Figure 1. Analysing device (a) with section view (b)

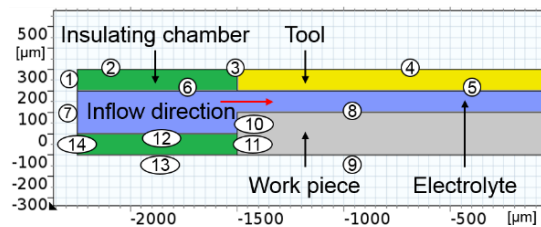


Figure 2. Detail of the 2D model geometry built up in COMSOL Multiphysics

The figure shows a detailed view of the 2D-model of the analysing device. The model includes merely the parts which are relevant for the electrochemical dissolution. These relevant parts are the tool electrode as cathode (highlighted in yellow), the work piece as anode (grey), the electrolyte canal (blue) and the surrounding insulating chamber (green).

The tool and the work piece have a diameter of 3000 μm. The working distance is 100 μm and the distance between upper and lower part of the chamber is 200 μm. The electrolyte flows in on the left side and flows out on the right side.

2.2 Physics

The developed fully coupled models use electric currents, non-isothermal flow and the deformed geometry interface.

In a first study the non-isothermal electrolyte flow was simulated with respect to the electrical current. This study was used to find parameters for the electrolyte flow and to determine whether the temperature of the electrolyte is constant. In this study the physics electric currents and non-isothermal flow are used.

Steel AISI 304 (stainless steel 1.4301) was chosen for the domain of the tool electrode and aluminium alloy EN AW 2017 was chosen for the work piece. For the aluminium alloy values of electric conductivity, thermal conductivity and heat capacity were added manually from a datasheet. [5] The domain of the electrolyte was assigned to water from the material library and defined with a conductivity typical for ECM, which is 7 S/m. The boundary conditions of the electric current interface according to figure 2 are listed in table 1.

Table 1: Boundary conditions according to figure 2 for the first study

Boundary	Definition
1-3	electric insulation
4	$U = 0 \text{ V}$
5	wall
6	electric insulation; wall
7	$u_0 = v_{inlet} \text{ [m/s]}$
8	wall
9	$U = 5 \text{ V}$
10	wall
11-12	electric insulation; wall
13-14	electric insulation

The boundary conditions used in this study are electric insulation, ground, electric potential, inlet an outlet of fluid and wall. The cathode surface on boundary 4 is set to the electric ground, which means a voltage of 0 V and the work piece is imposed on the anodic potential of 5 V on boundary 9. The boundaries 1 to 3, 6 and 11 to 14 have been assigned to the electrical insulation. The boundaries 5, 6, 8, 10 and 12 have been assigned to wall as a boundary of the electrolyte canal.

A second study was done to simulate the dissolution of the work piece. In this study the physics electric currents and deformed geometry are used. The electrolyte flow was not taken into

account for this study. The boundary conditions according to figure 2 are listed in table 2.

Table 2: Boundary conditions according to figure 2 for the second study

Boundary	Definition
1-3	$\vec{n} \cdot \vec{j} = 0$
4	$U = 0 \text{ V}$
5-7	$\vec{n} \cdot \vec{j} = 0$
8	$\vec{v}_n = V_{sp} \cdot \vec{j}_n$
9	$U = 5 \text{ V}$
10	$\vec{v}_n = V_{sp} \cdot \vec{j}_n$
11-14	$\vec{n} \cdot \vec{j} = 0$

The boundary conditions used in this study are electric insulation, ground, electric potential and prescribed mesh velocity. The settings for electric currents are similar to the setting in the previous study. With deformed geometry the dissolution was simulated. Only the boundaries 8 and 10 as work piece surfaces were given a prescribed mesh velocity, which relies on Faraday's law (equation 1). Faraday's law describes the functional principle of ECM. [6–8]

$$V = \frac{M}{\rho \cdot z \cdot F} \cdot Q = V_{sp} \cdot Q \quad (1)$$

V is the dissolved volume which depends on the molar mass M , the density ρ , electrochemical valence z of the material of the work piece. F is the Faraday constant and Q the electric charge transport. The first term can be written as specific dissolve volume V_{sp} . Equation 1 can be converted to equation 2, which is the velocity of material removal in normal direction \vec{v}_n as a function of the current density in normal direction \vec{j}_n . [9]

$$\vec{v}_n = V_{sp} \cdot \vec{j}_n \quad (2)$$

The used values to calculate the specific dissolve volume V_{sp} are listed in table 3.

Table 3: Values used to calculate V_{sp}

Symbol	Name	Value
M	Molar mass	28.77 g/mol
z_A	Valency	2.7
ρ	Mass density	2.8 g/cm ³
F	Faraday constant	96.49 · 10 ³ C/mol

2.3 Meshing

The FEM meshes that were used in the simulation were created using the automatic mesh creator.

For the first study to simulate the electrolyte flow, a mesh was generated, which is shown in figure 3. This mesh was used to evaluate the electrolyte flow and the temperature distribution.

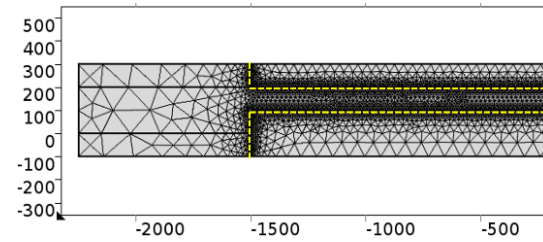


Figure 3. FEM mesh for the simulation of electrolyte flow and temperature distribution

The shown mesh was generated as a user-defined mesh with the settings “Extremely coarse” of “General physics” in the areas of solids and “Coarser” of “Fluid dynamics” in the area of the electrolyte. This mesh is generated as a free triangular mesh. A corner refinement and a boundary layer was added to the area of electrolyte (yellow line) to have a better resolution of fluid dynamics at the interface solid to fluid. The minimum element size in the solid areas is 225 μm and the maximum size is 1490 μm . The elements in domain of the fluids have a minimum size of 1.6 μm and a maximum size of 34.8 μm . The generated mesh consists of 4438 elements.

To simulate the electrochemical removal another mesh was generated, which is shown in figure 4.

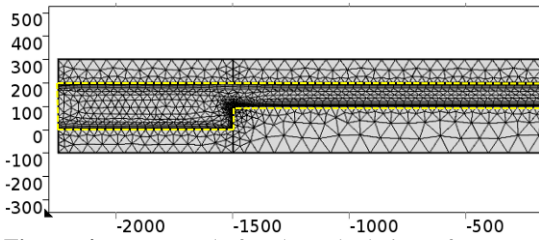


Figure 4. FEM mesh for the calculation of current density and electrochemical removal

To generate this mesh a user-defined mesh with the setting “Normal” in “General physics” for the entire model and a refined mesh along the boundaries of the tool and the work piece (yellow line) were chosen. The type of the mesh is a free triangular mesh. The areas with the setting “Normal” include minimum element size of $1.35 \mu\text{m}$ and a maximum element size of $302 \mu\text{m}$. In the refined areas the settings are based on the predefined setting “Extremely fine” and the maximum element size was set manually to $10 \mu\text{m}$. The generated mesh consists of 11369 Elements. These settings ensure an adequate fine resolution for the areas in which the current density and the electrochemical removal are calculated.

3. Results of the simulation

As mentioned above the simulation was divided into two studies. In the first study the electrolyte flow was simulated stationary and in the second study the electrochemical removal

was simulated transient. The results are presented in the following sections.

3.1 Electrolyte flow

To find appropriate parameters for the velocity of the electrolyte a parameter sweep of v_{inlet} was used for the simulation. The inlet velocity was set between 7.5 and 25 m/s with an increment of 1.25 m/s. A plot of the velocity magnitude and the velocity field for $v_{inlet} = 25 \text{ m/s}$ of the electrolyte is shown in figure 5. The arrows represent the velocity field. The electrolyte flows in on the left side with the set value of 25 m/s. The canal gets smaller at the x-value of -0.15 mm where the tool and the work piece are located. Near this narrowing the highest values of velocity with 64.3 m/s can be detected. After a levelling until an x-value of approximately -0.05 mm a parabolic flow profile has formed with the highest values of velocity in the centre of the canal. At the end of the work piece at $x = 0.15 \text{ mm}$ the lowest velocities can be detected at the bottom of the canal. Turbulences have to be expected after the narrowing at $x = -0.15 \text{ mm}$ and after the widening at $x = 0.15 \text{ mm}$. Figure 6 shows the maximal velocity and the velocity in the centre of the canal as a function of the inlet velocity.

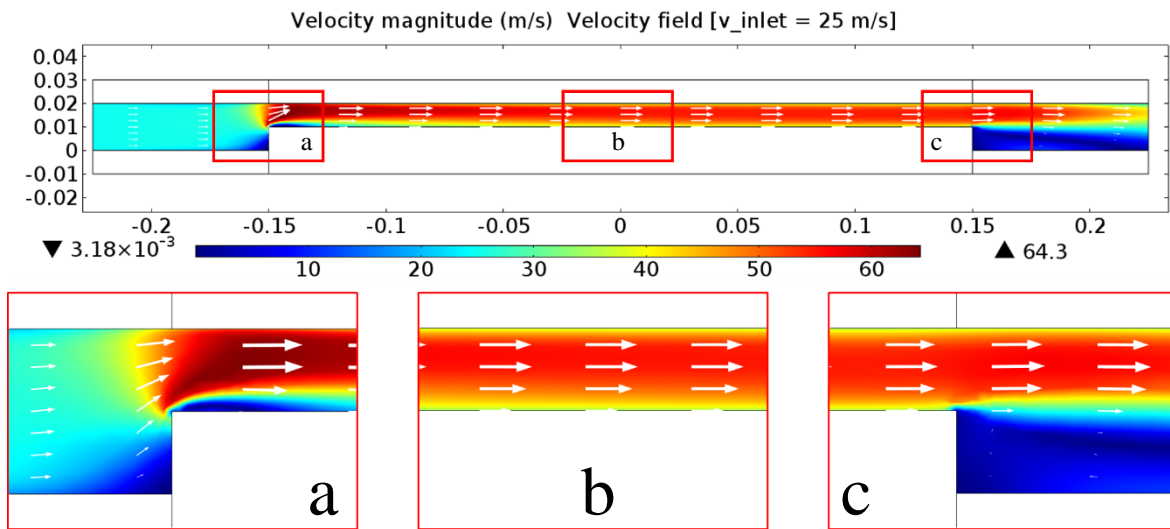


Figure 5. False colour rendering of the velocity magnitude and arrows of the velocity field for $v_{inlet} = 25 \text{ m/s}$

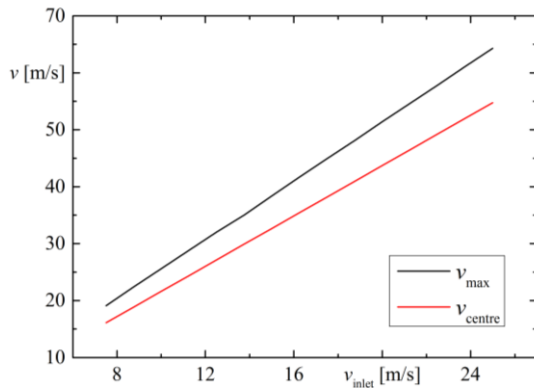


Figure 6. Maximal velocity v_{max} and velocity in the centre of the canal v_{centre} as a function of the inlet velocity

The maximal velocity (black line) and the velocity at the centre (red line) increase linearly with increasing inlet velocity. The velocity in the centre is approximately twice the inlet velocity.

The temperature was analysed because a homogeneous temperature distribution is aimed for the analysing process. With higher temperature the electric conductivity rises and the current density is influenced. Figure 7 shows the maximal temperature in the canal as a function of the inlet velocity.

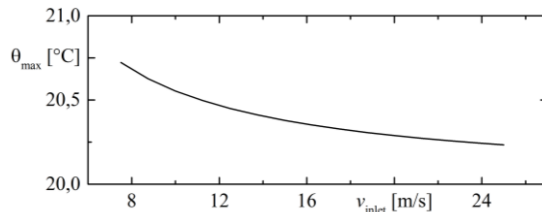


Figure 7. Maximal temperature in the canal as a function of the inlet velocity

The electrolyte flows in with a temperature of 20°C. Due to joule heating in the device the temperature increases. Because of the electrolyte flow the maximal temperature is limited. The maximal temperature decreases digressively with increasing inlet velocity. So the highest temperature is found at a low velocity. The difference to the initial temperature is in all studies less than 1 K. This result indicates that the chosen inlet velocities are suitable to establish a nearly constant temperature during the analysing process.

3.2 Electrochemical removal

In the second study the electrochemical removal of the work piece was simulated

transient. The simulation time was 1 s. As mentioned above, the dissolution was implemented by deformed geometry. To ensure a stable simulation, the option automatic remeshing was used. Because of the deformed geometry the values, e.g. of the current density were calculated for every time-step. In figure 8 the result of the transient calculation of the current density is shown for different time-steps by means of a false colour rendering. Additionally the deformed geometry can be seen.

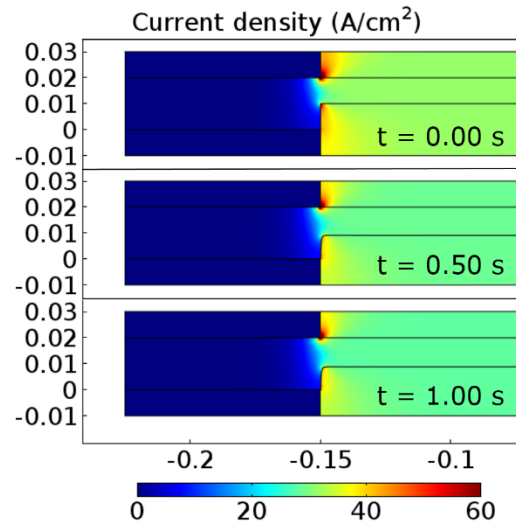


Figure 8. Transient calculation of current density and electrochemical removal for time-steps $t = 0$ s; 0.5 s and 1 s (limited to 60 A/cm²)

The figure shows the current density in half of the model for different time-steps. The magnitude of the current density was limited to 60 A/cm² in the images, higher values up to 220 A/cm occur. It can be seen that there is a current density of 0 in the insulating parts and in the electrolyte distant from tool and work piece. The highest values of the current density are located at the edges of tool and work piece. Due to this fact the highest rate of dissolution is localised at the edges. This high localisation leads to an edge rounding. Figure 9 shows the shape of the edge of the work piece for different time-steps.

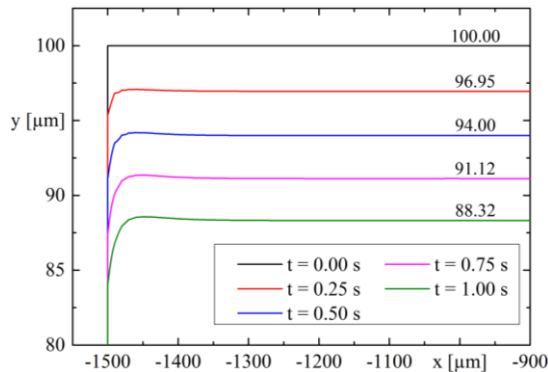


Figure 9. Shape of the edge of the work piece for time-steps $t = 0$ s; 0.25 s; 0.5 s; 0.75 s and 1 s

For every time-step another shape can be seen. The electrochemical removal increases with increasing time. It can be seen that there is an area near the edge, which is always higher than the value reached in the centre. The difference between those two heights is less or equal $0.25 \mu\text{m}$. After a simulated time of 1 s the height of the work piece has been reduced by approximately $12 \mu\text{m}$. Therefore, a feed rate applied to the analysing device towards the work piece theoretically can be up to $12 \mu\text{m/s}$ without colliding. The electrochemical removal with electrode feed differs from the static dissolution simulated in this study. Due to this fact the electrode feed will be added in a prospective study.

4. Summary

In this study multiphysics simulations of an analysing process to characterize the electrochemical removal of aluminium matrix composites were shown. Therefore, two coupled models of the developed analysing device were built up. The used physics are electric currents, non-isothermal flow and the deformed geometry interface.

In a first study the electrolyte flow was investigated without considering a deformed geometry. In this study the velocity field could be analysed. Furthermore the chosen inlet velocities establish a nearly constant temperature during process.

The anodic dissolution was simulated in the second study. Therefore, electric currents and deformed geometry interface were used. Based on Faraday's law the simulation leads to the result that there is an edge rounding of the work piece. The height of the deformed work piece is

approximately $12 \mu\text{m}$ less the height of the initial work piece after a simulated time of 1 s. So theoretically a feed rate of $12 \mu\text{m/s}$ can be applied to the device towards the work piece without colliding under the investigated process parameters.

The simulation leads to a better understanding of the processes in the analysing device. Furthermore, some settings for the analysing device, e.g. the inflow velocity of the electrolyte, were detected.

An enhancement of the model can be done by adding a feed rate of the analysing device towards the work piece. The behaviour of the electrolyte with respect to the deformed geometry should be investigated too. Prospectively a simulation of the analysing device with a 3D-model should be done to examine electrolyte flows more exactly.

Acknowledgements

The authors acknowledge the DFG (German Research Foundation) for supporting this work carried out within the framework of project CRC 692 HALS.

References

- [1] W. D. J. Callister, *Materials Science and Engineering: An Introduction, 7th Edition*. Wiley Publishers, 2006, p. 832.
- [2] R. Teti, "Machining of Composite Materials," *CIRP Ann. - Manuf. Technol.*, vol. 51, no. 2, pp. 611–634, Jan. 2002.
- [3] F. Müller and J. Monaghan, "Non-conventional machining of particle reinforced metal matrix composites," *J. Mater. Process. Technol.*, vol. 118, no. 1–3, pp. 278–285, Dec. 2001.
- [4] K. Hockauf, L. Köhler, M. Händel, T. Halle, D. Nickel, G. Alisch, and T. Lampke, "The effect of anodic oxide coating on the fatigue behaviour of AA6082 with an ultrafine-grained microstructure," *Materwiss. Werksttech.*, vol. 42, no. 7, pp. 624–631, Jul. 2011.

- [5] Gleich Aluminium, “EN AW 2017,” 2013.
- [6] A. Schubert, M. Hackert, and G. Meichsner, “Simulating the Influence of the Nozzle Diameter on the Shape of Micro Geometries Generated with Jet Electrochemical Machining,” in *Proceedings of the European COMSOL Conference, 2009*.
- [7] M. Hackert, G. Meichsner, S. Jahn, and A. Schubert, “Investigating the Influence of Dynamic Jet Shapes on the Jet Electrochemical Machining Process,” in *Proceedings of the European COMSOL Conference, 2010*.
- [8] M. Hackert-Oschätzchen, M. Kowalick, G. Meichsner, A. Schubert, B. Hommel, F. Jähn, M. Scharrnbeck, R. Garn, and A. Lenk, “2D Axisymmetric Simulation of the Electrochemical Finishing of Micro Bores by Inverse Jet Electrochemical Machining,” in *Proceedings of the European COMSOL Conference, 2013*.
- [9] M. Hackert-Oschätzchen, S. F. Jahn, and A. Schubert, “Design of Electrochemical Machining Processes by Multiphysics Simulation,” in *Proceedings of the European COMSOL Conference, 2011*.